

SINERGI Vol. 27, No. 3, October 2023: 405-414 http://publikasi.mercubuana.ac.id/index.php/sinergi http://doi.org/10.22441/sinergi.2023.3.011



Application of Capacity Spectrum Method (CSM) for nonsymmetrical reinforced concrete high-rise buildings as a tool for seismic design



Ayuddin^{1*}, K. R. Bindhu²

¹Department of Civil Engineering, Faculty of Engineering, Universitas Negeri Makassar, Indonesia ²Department of Civil Engineering, Faculty of Engineering, College of Engineering Trivandrum, India

Abstract

The development of earthquake resistance design of structures in the last decade has been critically changing from strength and ductility to performance criteria, where the structure is decided for various levels of structural performance. To understand the structural performance because, at time, a large earthquake load on the structure will experience structural yielding, non-linear analysis with the capacity spectrum method will be performed. The relationship between roof displacement and base shear force is described by a curve that describes the structural capacity is a capacity curve. To determine the behavior of the structures under review for a given earthquake intensity, the capacity curve is then compared with the performance demand based on various earthquake intensities. The results of the case studies for reinforced concrete portals nonsymmetrical 3D concluded that the convergence obtained at the point of the structure performance is $a_p = 0.236g$ and $d_p = 189 m$. The displacement results for the actual structure (Δ_{roof}) were 286.71 mm and building base shear coefficient was 15.46 %.

his is an open access article under the CC BY-SA license



Keywords:

Capacity spectrum method; Performance based design;

Article History:

Received: March 15, 2023 Revised: May 29, 2023 Accepted: June 4, 2023 Published: October 2, 2023

Corresponding Author:

Ayuddin

Civil Engineering Department, Universitas Negeri Makassar, Indonesia

Email: ayuddin@unm.ac.id

INTRODUCTION

Indonesia is a zone region that often experiences and the earthquake, so buildings will be built must be able to survive when an earthquake occurs [1][2]. The effect of an earthquake on reinforced concrete buildings is always carried out even studies on the influence of ground motion patterns that cause a shift in a building [3]. The building was built with reinforced concrete, which caused damage to buildings due to earthquakes. Reinforced Concrete (RC) buildings with no seismic design exhibit degrading behavior under severe seismic loading owing to nonductile brittle failure modes [4][5]. special engineering firms have used performance based seismic design for rehabilitation [6]. Thus, the damage that occurs most often owing to design errors and the quality of materials is very low. Current codes and provisions cannot cover all structures located in active seismic zones, and these structures cannot withstand seismic action [7]. Finally, the overall seismic safety of a building suffers from the level of damage observed from the deformation capacity that occurs [8].

Recent developments in structural design philosophy have tended to focus on performance-based design concepts. This method is oriented to the performance required for future user needs of a building and then evaluates and verifies the building assets [9]. Probabilistic Seismic Analysis, which is often implemented in the first generation of performance based seismic engineering, quantifies the seismic behavior of structures with the desired demand parameters considering all anticipated earthquakes [10].

Structural Engineers realize that structural safety does not merely depend on the quantitative strength, but also on the performance-based ductility demand and energy dissipation involving the corresponding major earthquake. An improved

capacity-demand diagram method that uses the well-known constant-ductility design spectrum for the demand diagram was developed and illustrated by examples [11].

Performance Based Design (PBD), primarily based on ductility demand under major earthquakes, has been considered as a criterion for measuring the safety of a structure. Seismic performance evaluation of steel buildings with oil dampers was performed using the capacity spectrum method [12][13]. This performancebased design uses nonlinear analysis techniques based on computers to analyze various ground motion intensities, and an approach based on approaches based on the equivalent linearization concept of the capacity spectrum [14, 15, 16]. Thus, it can be seen in a critical condition performance and it can be anticipated that it does not meet the necessary requirements. ATC-40 rules were applied in this study to determine the performance of the building structure because the rules did not formulate the equation SNI 1726-2002.

To verify the structural performance in a nonlinear manner, nonlinear static analysis is required to predict the lateral displacement accurately and conservatively. One way of nonlinear static analysis has been proposed that the most popular today is the Capacity Spectrum Method (CSM) [17].

The CSM is a nonlinear static analysis method, that which compares the global forcedisplacement capacity curve of a structure with an earthquake response spectrum in a graphical shape [18]. For this, both the capacity curve and the response spectra must be converted into a spectral acceleration Sa spectral displacement SD graph. Owing to this transformation, global buildings will be reduced to an equivalent SDF structure. Using a trial and error procedure, one can estimate the performance point, which describes the spectral displacement of the building due to a given earthquake [19]. Deformation has been used as a key indicator in seismic performance assessments of building structures [20].

MATERIAL AND METHODS Capacity Spectrum Method Procedure

The capacity spectrum method is a graph technique for determining the structural response by finding the intersection diagrams from the analysis of nonlinear static pushover and acceleration response spectra curves—displacement [21]. The analysis of a nonlinear pushover is a one component of performance-based design that can be used to determine the capacity of a structure [22][23]. The structure was

subjected to specified load pattern to reach the target displacement [24].

In the CSM method, the structural capacity curve (force vs. displacement) and response spectra curves are used [25, 26, 27]. It must be converted into acceleration spectra (SA) and displacement spectra (SD). The conversion pushover capacity curve was calculated based on the mass coefficients of the effective modal and modal participation factors because the CSM method is a combination of several techniques or procedures for seismic analysis, it will be too broad to discuss in detail. Therefore, the description below is given only a general description given in the method with the required number of equations. The procedure is summarized as follows.

Capacity Curve

Estimate or calculate the capacity curve in terms of roof displacement Δ_R and base shear, V, (i.e., total lateral force at the base). The capacity curve is determined by statically loading the structure with realistic gravity loads combined with a set of lateral forces to calculate the roof displacement Δ_R and base shear V, which define the first significant yielding of structural elements. The vielding elements were then relaxed to form plastic hinges and incremental lateral loading was applied until a nonlinear static capacity curve was created. The curve is created by the superposition of each increment of displacement, and includes tracking displacements at each story (ATC-40). This procedure is sometimes referred to as pushover analysis.

Dynamic characteristics

Estimate or calculate modal vibrational characteristics:

The Modal Participation Factor (Γ)

The Modal Participation Factor (MPF) was calculated for each vibration mode by using (1):

$$PF_m = \begin{bmatrix} \frac{\sum_{i=1}^{N} \frac{w_i \phi_{im}}{g}}{\sum_{i=1}^{N} \frac{w_i \phi_{im}^2}{g}} \end{bmatrix}$$
 (1)

Where:

 PF_m = Modal Participation Factor for mode to-

 $w_i \phi_{im}/g = \text{floor mass to-i}$

 ϕ_{im} = mode amplitude to-m for floor to-i N = floor N, The top floor of the structure Modal participation factor for certain floors (modal story participation factor):

$$PF_m = PF_m \phi_{im} \tag{2}$$

The Coefficient of Effective Mass (α_m)

The Coefficient of Effective Mass was calculated for each vibration mode using (3):

$$\alpha_m = \frac{\left[\sum_{i=1}^N \frac{w_i \theta_{im}}{g}\right]^2}{\left[\sum_{i=1}^N \frac{w_i}{g}\right] \sum_{i=1}^N \frac{w_i \phi_{im}^2}{g}} \tag{3}$$

The Modal Floor Acceleration (a)

The Modal Floor Acceleration was calculated for each vibration mode using (4):

$$a_{im} = PF_m \phi_{im} S_{Am} \tag{4}$$

Where:

 a_{im} = acceleration of the floor at the level to-i for the mode to-m

 ϕ_{im} = amplitude at the level to-i for the mode to-

 S_{Am} = spectra acceleration for the mode to-m

The Lateral force of modal floor F_{im}

The lateral force (mass x acceleration) is calculated for each vibration mode using (5):

$$F_{im} = PF_m \phi_{im} S_{Am} m_i \tag{5}$$

Where:

= floor lateral force to-i for the mode to-m F_{im}

= floor mass at the level to-i m_i

= spectra acceleration for the mode to-m S_{Am}

Modal Shear Force (V_m)

The Modal Shear Force is calculated for each vibration mode using (6), and the amount of lateral force floor F_{im} is equal to V_m :

$$V_m = \alpha_m S_{Am} M \tag{6}$$

Where:

= total lateral force for the mode to-m V_m

= Effective mass coefficient for the mode α_m

= structure total mass

Spectral capacity engineering applications that require response spectra and capacity curves are plotted in the format of acceleration-displacement (ADRS). Further below illustrates some of the parameters to determine the factors reducing the capacity spectra.

$$S_{di} = \frac{T_i^2}{4\pi^2} \, S_{ai} \, g \tag{7}$$

Modal Shear Force (V_m)

The Modal Participation Factor (MPF) was calculated for each vibration mode using (6). Modification of the damping factor (κ) is the size of the hysteresis behavior of the price of building. These parameters are determined by the assessment of the quality system structure under earthquake loads in a certain time interval. In this study, the structures were analyzed using the

lateral control system of the beam column resistant frame, Therefore the damping factor was modified as follows:

$$\kappa = 0.67, \beta_{eff} 25\%$$

$$\kappa = 0.845 - \frac{0.4461 (a_y d_{pi} - d_y a_{pi})}{a_{pi} d_{pi}} \beta_{eff}$$

$$> 25\%$$
(8)

$$a_{pi}d_{pi} \qquad \qquad P_{eff}$$

$$> 25\% \qquad (9)$$

Effective Damping (β_{eff})

Effective damping is a modified hysteresis damping with a damping modification factor (κ). While hysteresis damping is the damping refers to the damping of an inelastic structure. The common method used to determine the equivalent viscous damping is to balance the energy dissipation in a cycle of vibration of a system inelastic with an equivalent linear system in Figure 1.

Based on this concept, the ideal hysteresis damping is calculated as follows:

$$\beta_0 = \frac{1}{4\pi} \frac{E_D}{E_{S_0}} \tag{10}$$

Where:

 E_D = disipation of energy by damping

 E_{s_0} = the maximum strain energy

From the broad equality of calculation E_D dan E_{s_0} , the equivalent viscous damping (hysteresis damping) is given as:

$$\beta_0 = \frac{63.7\kappa (a_y d_{pi} - d_y a_{pi})}{a_{pi} d_{pi}} \tag{11}$$

Taking into account the viscous damping inherent in reinforced concrete structures by 5% so the total equivalent viscous damping:

$$\beta_{eq} = \beta_0 + 5 = \frac{63.7\kappa(a_y d_{pi} - d_y a_{pi})}{a_{pi} d_{pi}} + 5$$
 (12)

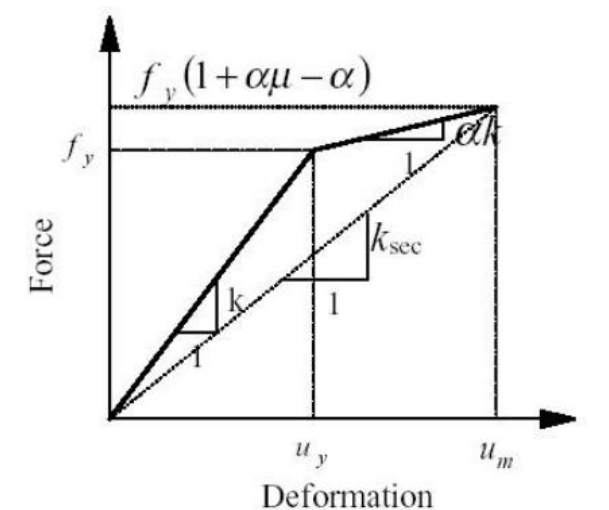


Figure 1. Equivalent viscous damping relation hysteresis energy dissipation

The modification factor should be modified given to calculate imperfect hysteresis loops so that the effective structural damping is expressed in (12) (β_{eff}) .

Acceleration reduction factor (S_{RA}) and Velocity reduction factor (S_{RV})

In this capacity spectrum method, the reduction factors for the equivalent elastic system are given as:

$$SR_A = \frac{3.21 - 0.68 \ln(\beta_{eff})}{2.12} \tag{14}$$

$$SR_A = \frac{3.21 - 0.41 \ln(\beta_{eff})}{1.65} \tag{15}$$

Capacity spectra peak acceleration (SA) and Angle period (TS):

Capacity spectra peak acceleration related hearing with *trial performance point* a_{pi} , d_{pi} , given as:

$$S_A = 2.7065 S_{RA} C_A \tag{16}$$

"(Equation 16)" using factor "2.7065" because responsive design spectra constructed using Newmark-Hall procedure. When using the design response spectrum normalized average factor "2.5" is used (ATC-40). Capacity spectra angle period is given:

$$T_S = \frac{S_{RV}C_V}{2.5 \, S_{RA}C_A} \tag{17}$$

Determining the loading capacity of the Lateral Displacement Structure (Non-Linear Static Pushover Analysis)

After the configuration of static lateral load was applied to the structure, the intensity gradually increased (push-over). Capacity curve is then generated as the structure of the scheme is

shown in Figure 2. The Pushover curve should be determined by 4 points (Point A - Point D) which represent the relationship between roof floor displacement (Δ_{roof}) and lateral shear force (V).

Pushover capacity curves conversion and Spectra Response AT

To superimpose structure capacity diagram on diagram spectra so abscissa (X-axis and Y axis) in pushover capacity and Spectral response curve must be converted to spectrum displacement (SD) and spectra acceleration (SA). The transformation of the structure capacity curve using (1) and (2) in shown in Figure 3. The transformation of this response spectra using (7) and shown in Figure 4.

Each point on the spectrum response curve represents the unique values of the acceleration spectra, S_{ai} , velocity, S_{vi} , and dispacement, S_{di} . To change the spectra from conventional form S_A vs T become ADRS form S_A vs T to the ADRS form, every point on the curve SA vs. T needs to be changed to SD.

Determine the point of structural performance

Performance Point is determined by plotting the capacity diagram and the amount of spectrum capacity of ADRS format. The capacity diagram intersection and spectrum capacity of a damping value represents a strong demand on the structural response due to lateral earthquake loading. The point performance calculation process is basically the procedure trial and error mode or uses a graphical approach, as shown in Figure 5.

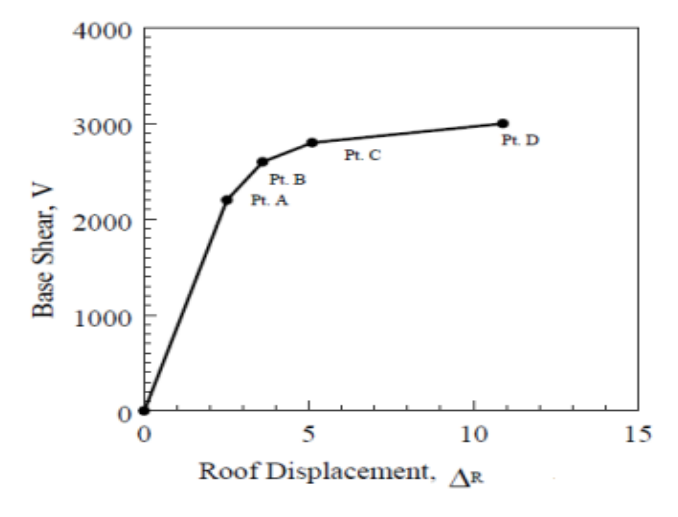
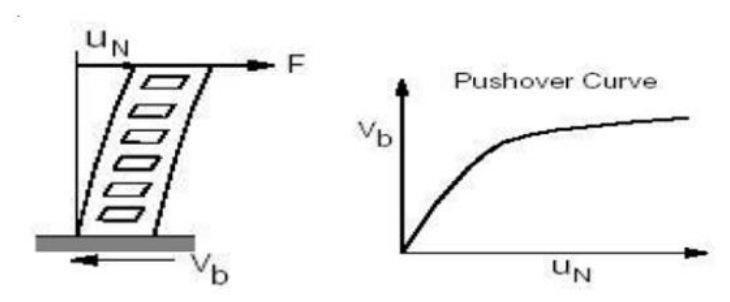
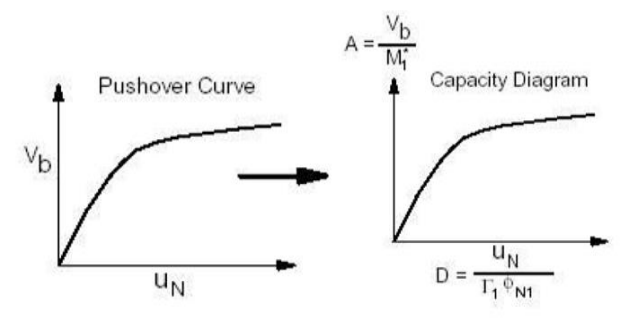


Figure 2. Capacity Curve with the performance point



(a). Shear force relationship curve - displacement



(b) Capacity transformation curve to capacity Figure 3. Capacity spectra method: Capacity curve transformation

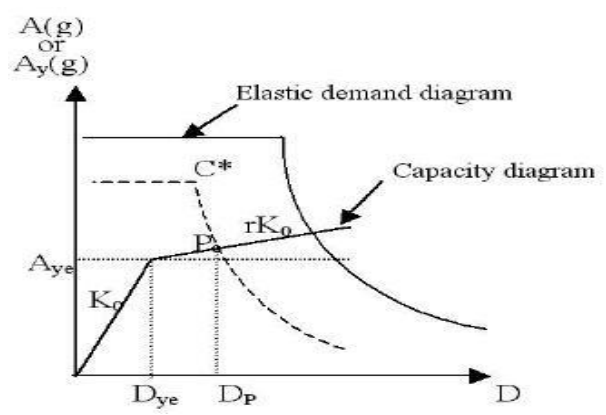


Figure 4. Spectra capacity Method: Response spectra conversion

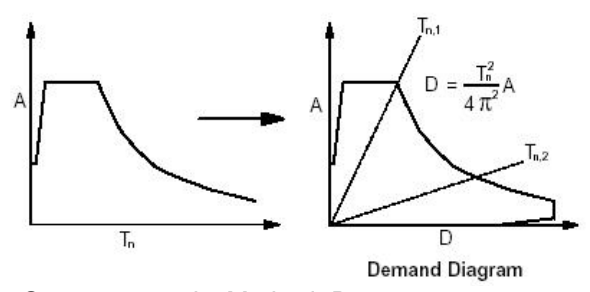


Figure 5. Spectra capacity Method: Response spectra conversion

Method

The method used in this research is to analyze with design parameters of reinforced concrete structure non-symmetric with three-dimensional portal review can be seen in Figure 6 below. Structural dimensions: 4@8m x 3@8 in plane and 3m in height for each story, fc'=30 Mpa

and F_y = 350 MPa. Table 1 presents a section of the building structural elements. Typically, all storeys of the building have constant three meters height. These structures were analyzed using the spectrum capacity method.

Table 1. Detail of the Frame Structure

| Description of Asymmetrical Building | Member Used |
|---------------------------------------|-------------|
| Number of Storeys | 8 |
| Number of Grid Lines in X - Direction | 4 |
| Spacing of Grids in Y-Direction (m) | 8 |
| Bottom Storey Height (m) | 4 |
| Typical Storey Height (m) | 3.6 |

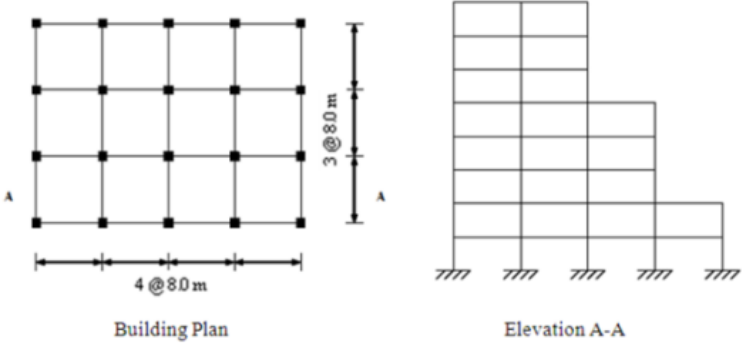


Figure 6. Typical Building Plan

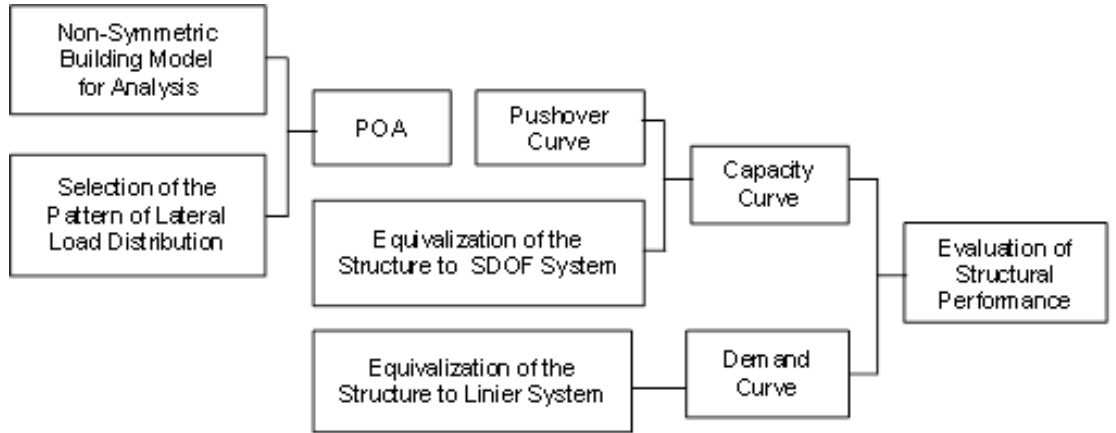


Figure 7. The Procedure chart of the analysis by method of capacity demand curve

In this analysis will be found an intersection between the demand curve and the capacity curve for the largest top displacement. The main procedure of the analysis is shown in Figure 7.

RESULTS AND DISCUSSION

In the analysis of the asymmetric building under review, the calculation of dynamic characteristics is carried out using the principle of mass distribution in the structure of the software application, which is shown in Table 2 and the calculation of dynamic characteristics is also completed using the Lumped Mass principle, known as the Holzer or Stodola method, which is shown in Table 3. The distribution of static seismic forces on the joints is presented in Table 4. The distribution of lateral static forces along the height of the building of mass and height of each floor is shown in Figure 8.

Table 2. Distributed Mass Vibration Mode

| Mode | 1 | 2 | 3 | 4 | 5 | 6 | 7 | 8 |
|---------------------------|-------|-------|-------|-------|-------|-------|----------|------|
| Vibration Period, T (sec) | 0.933 | 0.864 | 0.753 | 0.45 | 0.413 | 0.379 | 0.397 0. | .342 |
| Ratio Vibration, T/Tm | 1.000 | 0.916 | 0.816 | 0.479 | 0.425 | 0.407 | 0.386 0 | .357 |

Table 3. Lumped Mass Vibration Mode

| Table 6: Earriped Mass Vibration Mede | | | | | | | | |
|---------------------------------------|-------|-------|-------|--|--|--|--|--|
| Mode | 1 | 2 | 3 | | | | | |
| Vibration Period, T (Sec) | 0.915 | 0.856 | 0.743 | | | | | |
| Vibration Period Ratio, T/Tm | 1.000 | 0.912 | 0.813 | | | | | |

Table 4. Distribution of Static Seismic Forces on the Joints

| | | | Column | Midspan | Midspan | Endspan | Endspan |
|--------|---------|--------------------|--------------------|---------|---------|---------|---------|
| ω | Fi (kN) | Beam | | Frame | Frame | Frame | Frame |
| STOREY | | Dimension | Dimension | Front/ | | Front/ | |
| Ĕ | | , b x h, <i>mm</i> | , b x h, <i>mm</i> | Back | Center | Back | Center |
| | | | | Joint | Joint | Joint | Joint |
| 1 | 241.43 | 500x900 | 700x700 | 10.65 | 17.35 | 7.27 | 10.47 |
| 2 | 514.35 | 500x900 | 700x700 | 24.01 | 37.26 | 14.37 | 24.02 |
| 3 | 631.67 | 500x800 | 600x600 | 38.49 | 64.02 | 24.09 | 39.98 |
| 4 | 952.75 | 500x800 | 600x600 | 55.36 | 91.51 | 34.59 | 56.37 |
| 5 | 1208.32 | 500x800 | 600x600 | 69.76 | 112.49 | 43.83 | 71.49 |
| 6 | 1008.41 | 500x700 | 500x500 | 83.05 | 142.95 | 52.29 | 83.1 |
| 7 | 1137.06 | 500x700 | 500x500 | 97.49 | 163.18 | 57.27 | 97.76 |
| 8 | 1146.22 | 500x700 | 500x500 | 97.27 | 163.85 | 59.09 | 97.42 |
| Σ | 6840.21 | | | | | | |

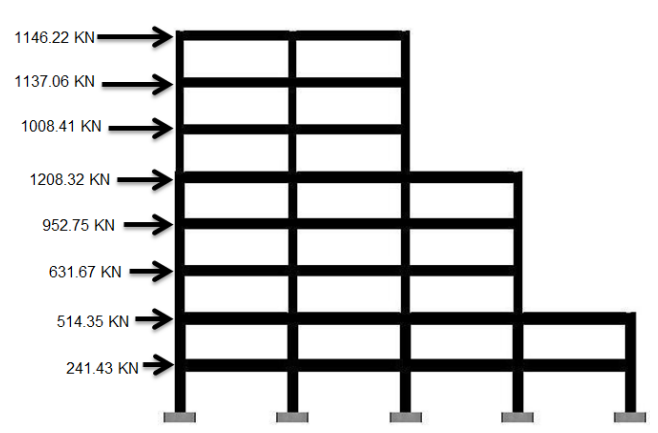


Figure 8. Static Earthquake Diagram for each Floor

From the application of the design total base shear force Vb = 6840.21 KN which is distributed over 124 joints with the load intensity increasing gradually through pushover analysis, the displacement capacity curve of the structure is produced as shown in Figure 9.

Table 5 provides information about the displacement behavior and base shear force that occur in each pushover steps carried out through the ETABS software structure. The capacity analysis did not indicate the collapse mechanism or plastic joint destruction occurred only at the bottom of the column base floor. This means that the structural design accommodated the capacity concept of weak beam-strong column. The

maximum performance of the structure, Δ_{maks} is 792 mm, and the next stage is shown in Figure 10.

At point A (V= 5100 KN, $\Delta=216$ mm) indicates the beginning of the plastic hinge mechanism, and at point B (V= 6300 KN, $\Delta=279$ mm) initial failure occurs on some structural elements. Point C (V= 7450 KN, $\Delta=525$ mm) occurs at the midpoint of strain hardening. For point D (V= 8550 KN, $\Delta=792$ mm) the displacement limit occurs where the structure is on the verge of collapse or is undergoing local collapse, reaches maximum curvature.

Table 5. Structural Capacity in Displacement and Base Shear Force and Base Shear Force

| Step | Displacement | Base Force | A-B | B-IO | IO-LS | LS-CP | CP-C | C-D | D-E | >E | TOTAL |
|------|--------------|------------|-----|------|-------|-------|------|-----|-----|----|-------|
| 0 | 0.000 | 0.000 | 394 | 0 | 0 | 0 | 0 | 0 | 0 | 0 | 394 |
| 1 | 0.092 | 2215.162 | 394 | 0 | 0 | 0 | 0 | 0 | 0 | 0 | 394 |
| 2 | 0.184 | 4308.713 | 394 | 0 | 0 | 0 | 0 | 0 | 0 | 0 | 394 |
| 3 | 0.216 | 5150.242 | 399 | 2 | 0 | 0 | 0 | 0 | 0 | 0 | 394 |
| 4 | 0.283 | 6397.568 | 299 | 98 | 0 | 0 | 0 | 0 | 0 | 0 | 394 |
| 5 | 0.297 | 6397.568 | 292 | 107 | 0 | 0 | 0 | 0 | 0 | 0 | 394 |
| 6 | 0.385 | 6903.128 | 278 | 68 | 68 | 0 | 0 | 0 | 0 | 0 | 394 |
| 7 | 0.489 | 7421.945 | 254 | 89 | 36 | 53 | 0 | 0 | 0 | 0 | 394 |
| 8 | 0.721 | 8162.457 | 213 | 58 | 62 | 78 | 0 | 0 | 0 | 0 | 394 |
| 9 | 0.861 | 8486.385 | 213 | 54 | 51 | 102 | 0 | 0 | 0 | 0 | 394 |
| 10 | 0.897 | 8926.863 | 213 | 39 | 57 | 107 | 0 | 8 | 0 | 0 | 394 |

Then, structure performance intersection results can be seen in Figure 11.

The performance point was derived from the intersection diagram of capacity structure and spectra capacity curve. The results of the spectrum capacity method in Figure 11 shows that the convergence performance derived at the structure performance point, a_p is 0.23g and displacement spectra is 189 mm. Based on the displacement spectra, the actual displacement of the structure was 286.71 mm and the building base shear coefficient was 15.46 %.

Figure 10 shows the stages of performance that occur in a structure and are shown step by step. The four performance points on the capacity

curve shown in the force vs displacement curve represent a stage up to the threshold of collapse. At point A is the beginning of a plastic hinge mechanism by starting an incident on the upper floor of the building. At point B begins the occurrence of a local collapse on some structural elements, this indicates that the mechanism stage has begun to occur. At point C is the point where strain hardening occurs. Meanwhile, at point D is the occurrence of a maximum performance structure that is on the verge of collapse. Then further shows that the maximum performance of the structure that occurs is in the position Δ_{maks} 792 mm.

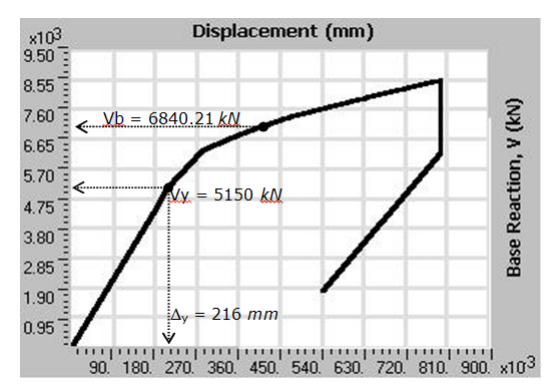


Figure 9. Vertical Non-Symmetric Structural Capacity Curve (V vs Δ)

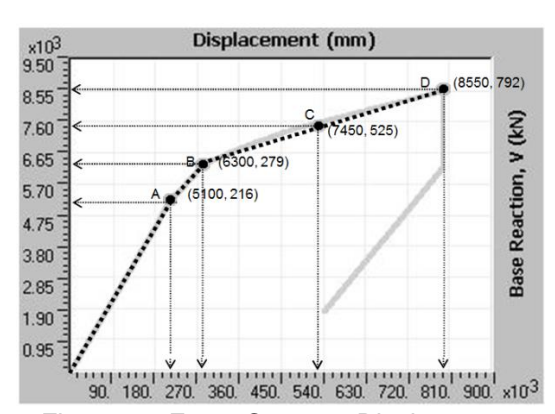


Figure 10. Force Curve vs Displacement

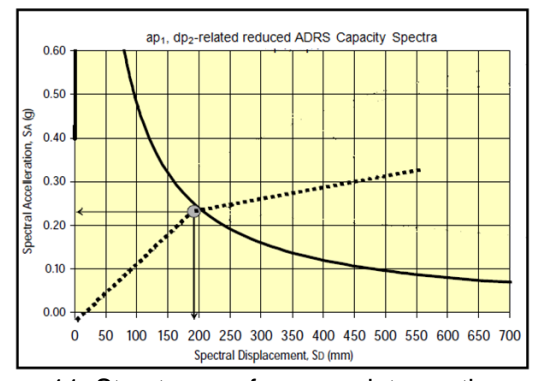


Figure 11. Structure performance intersection result

The concept of structure performance design the CSM is basically a performed to obtain the actual displacement of the building structure. The actual displacement obtained from these results show a structure the floor displacement. Thus, this method can be used as an alternative design of seismic resistance structure.

The advantage of the CSM method is that it does not require the determination of specific basic parameters. Thus, according to the results of the studies on irregular high-rise buildings published in this article, this CSM method can accommodate various types and configurations of structures, including irregular structures. This article displays some information about the performance points shown in the capacity curve in Figure 9. Thus, it can be seen that the maximum performance of an irregular structure approaches collapse [26][27]. Furthermore, the results of this CSM analysis did not indicate the occurrence of local collapse in the structure being reviewed. These results indicate the need for this article as a reference for future on different analytical methods.

CONCLUSION

The results for the non-symmetric reinforced concrete structure in this study are in Occupancy of Immediate category performance level. This implies that the structure was designed to secure the conditions. Thus, the CSM can demonstrate the performance of a seismic resistance structure. The results of the analysis using the CSM method showed that there was no local collapse mechanism on the ground floor columns. These results indicate that the structural design accommodates the weak beam strong column concept. The capacity curve generated in the CSM method is a representation of the stages in which the plastic hinge mechanism begins to form, the global elastic limit of the structure, the center point of strain hardening, and the maximum performance limit where the structure approaches collapse.

ACKNOWLEDGMENT

The author would like to thank for all member of the Universitas Negeri Makassar especially for Civil Engineering Department for their support in this paper.

REFERENCES

[1] Ayuddin, "Global Structural Analysis of High Rise Hospital Building Using Earthquake Resistant Design Approach," *SINERGI*, vol. 24, no. 2, February 2020, pp: 95-108, doi: 10.22441/sinergi.2020.2.003.

- [2] Ayuddin, *Konstruksi Tahan Gempa*, Badan Penerbit UNM, Indonesia, 2017.
- [3] A. Faisal, A. Anshari, B. Hadibroto, and A. F. Kamaruddin, "Seismic Performace of Moment Frames Under Multiple Fling-Step Pulse Ground Motions," SINERGI, vol. 26, no. 2, June 2022, pp: 155-164, doi: 10.22441/sinergi.2022.2.004.
- [4] Ayuddin, Struktur Beton Bertulang, Indonesia, Badan Penerbit UNM, Indonesia, 2022
- [5] N. Kyriakides et al., "Evaluation of Seismic Demand for Substandard Reinforced Concrete Structures," The Open Construction and Building Technology Journal, vol. 12, pp. 9-33, 2018, doi: 10.2174/1874836801812010009.
- [6] B. Ahmed and S. M. Zahurul Islam, "Seismic Performance and Retrofitting of Steel Building," Science Publishing Group, vol 3, no. 1, January 2019, doi: 10.11648/j.ie. 20190301.11.
- [7] B. Ahmed, S. M. Z. Islam, "Seismic Performance and Retrofitting of Steel Building," *Industrial Engineering*, vol. 3, no. 1, 2018, pp. 1-10, doi: 10.11648/j.ie. 20190301.11.
- [8] C. Michel, A. Karbassi, P. and Lestuzzi, "Evaluation of the seismic retrofitting of a reinforced masonry building using numerical modeling and ambient vibration measurements," Article in Engineering Structures, vol. 158, pp. 124–135, March 2018, doi: 10.1016/j.engstruct.2017.12.016.
- [9] M. A. Zubritskiy, O. Y. Ushakov, L. S. Sabitov, "Performance-based seismic evaluation methods for the estimation of inelastic deformation demands," *IOP Conference Series: Materials Science and Engineering*, vol. 570, ID: 012108, 9 November 2020, doi: 10.1088/1757-899X/570/1/012108.
- [10] M. Kia, A. Amini, M. Bayat, and P. Ziehl, "Probabilistic Seismic Demand Analysis of Structures Using Reliability Approaches," *Journal of Earthquake and Tsunami*, vol. 15, no. 3, ID: 2150011, 2021, doi: 10.1142/S1793431121500111
- [11] K. Chopra, M. EERI and R. K. Goel, M. EERI, "Capacity Demand Diagram Methods Based on Inelastic Design Spectrum," *SAGE Journal*, vol. 15, no. 4, 27 December 2019, doi: 10.1193/1.1586065.
- [12] A. Naqi, T. Saito, Seismic Performance Evaluation of Steel Buildings with Oil Dampers Using Capacity Spectrum Method," *Appl. Sci.*, vol. 11, no. 6, pp. 2687, 2012, doi: 10.3390/app11062687.

- [13] G. Guerrini, S. Kallioras, S. Bracchi, and F. Graziotti, "Displacement Demand for Nonlinear Static Analyses of Masonry Structures: Critical Review and Improved Formulations," *Buildings*, vol. 11, no. 3, pp. 118, 2021, doi: 10.3390/buildings11030118.
- [14] Y. Lu, I. Hajirasouliha, A. M. Marshal, "Direct displacement-based seismic design of flexible-base structures subjected to pulselike ground motions," *Engineering Structures*, vol. 168, pp. 276-289, August 2018, doi: 10.1016/j.engstruct.2018.04.079
- [15] A. T. Dohadwala, R. K. Sheth, and I. N. Patel, "Comparison of Base Shear For Forced-Based Design Method And Direct Displacement-Based Design Method," *Int. J. Adv. Eng. Res. Dev.*,vol. 1, no. 06, pp. 1–10, 2018,
- [16] S. Swathi, K. Venkataramana, C. Rajasekaran, "Evaluation of Performance Point of Structure Using Capacity Spectrum Method," *Applied Mechanics and Materials*, vol. 877, pp. 299-304, February 2018
- [17] S. Swathi, K. Venkataramana, C. Rajasekaran, "Evaluation of Performance Point of Structure Using Capacity Spectrum Method," *Applied Mechanics and Materials*, vol. 877, pp. 299-304, February 2018
- [18] N. Ramadhani and A. Rosyidah, "Direct Displacement Based Design and Capacity Spectrum Method for Special Moment," Journal of Engineering Design and Technology, vol. 20, no. 1, pp. 6 – 12, March 2020
- [19] RFEM and RF-DINAM Pro, "Evaluate the Capacity Curve for Pushover Analysis," Dlubal Software GmbH Version January 2019, Germany, https://www.dlubal.com.
- [20] H. G. Kim and K. H. Kim, "A Simple Analysis Method for Estimation of Required Damping Ratio for Seismic Response Reduction," Journal of Asian Architecture and Building Engineering Taylor and Francis Group, vol. 17, no. 3, pp. 465-472, doi: 10.3130/jaabe.17.465.

- [21] A. V. Bergami, C. Nuti, D. Lavorato, G. Fiorentino, and B. Briseghella, "Proposal of a nonlinear static analysis procedure for bridges: the Incremental Modal Pushover Analysis for bridges (IMPAβ)," *Appl. Sci.*, vol. 10, pp. 4287, 16 February 2020, doi: 10.3390/app10124287.
- [22] Masrilayanti, R. Kurniawan, A. L. Budi, and S. H. Sourkan, "Pushover Analysis of 10-Floors Reinforced Concrete Building (Case study: Mahkota Majolelo Sati Bautique Hotel)," IOP Conference Series: Materials Science and Engineering, vol. 1041, ID: 012003, 2021, doi: 10.1088/1757-899X/1041/1/012003.
- [23] R. Patle, S. S. Shiwarkar, R. L. Gathe, A. V. Ghate, and M. P. Wandile, A. Bhambulkar, and V. Yerpude, "A Review On Pushover Analysis on RCC works," *International Journal of Advance Research and Innovative Ideas in Education*, vol. 7, no. 3, 2021.
- [24] A. Fakhraddini, M. J. Fadaee, and H. Saffari, "A Target Displacement for Pushover Analysis to Estimate Seismic Demand of Eccentrically Braced Frames," *Journal of Rehabilitation in Civil Engineering*, 14 July 2018, doi: 10.22075/JRCE.2018.13427. 1245
- [25] N. M. Rahbari, J. Dowling, D. Kennedy, and G. Fraser, "Comparison of Commonly-Used Pushover and Modal Pushover Analysis of Granville Bridge," 12th Canadian Conference on Earthquake Engineering, Quebec City, June 17-20, 2019.
- [26] S. Erlicher, O. Lherminier, and M. Huguet, "The E-Dva Method: A New Approach for Multi Modal Pushover Analysis Under Multi Component Earthquakes," Soil Dynamics and Earthquake Engineering, 1 May 2020,
- [27] A. Nurdini, E. Susila, T. Taufikurahman, N. F. Hadianto, M. Al Lubbu and A. Suryati, "Building a Prototype of an Eco-friendly House in the Peri-Urban Area," *Journal of Integrated and Advanced Engineering (JIAE)*, vol. 1, no. 1, pp. 21-28, 2021, doi: 10.51662/jiae.v1i1.9